A&A 410, 983–991 (2003)
DOI: 10.1051/0004-6361:20031327

Astronomy & Astrophysics

The rapidly rotating δ Scuti star AV Cetei*

T. H. Dall[1], G. Handler[2,3], M. B. Moalusi[4], and S. Frandsen[5]

[1] European Southern Observatory, Alonso de Cordova 3107, Casilla 19001, Santiago 19, Chile
[2] Institut für Astronomie, Universität Wien, Türkenschanzstrasse 17, 1180 Vienna, Austria
[3] South African Astronomical Observatory, PO Box 9, Observatory 7935, South Africa
[4] Department of Physics, University of the North-West, Private Bag X2046, Mmabatho 2735, South Africa
[5] Department of Physics and Astronomy, Aarhus University, 8000 Aarhus C, Denmark

Received 18 June 2003 / Accepted 22 August 2003

Abstract. We present results from an international spectroscopic and photometric campaign on the δ Scuti star AV Cet. The star has a rich and complex pulsation spectrum, and we find 7 individual frequencies, with evidence for many more present below our detection limit. We investigate the prospects for mode identification in fast rotators, using several different techniques. We compare the methods and conclude that although no single technique can give unambiguous mode identification, the collective evidence does allow some conclusions to be drawn, suggesting the presence of one radial mode at 14.598 d^{-1}. During the campaign we found the star HD 9139 to be a variable. From our photometry we find evidence for a variability time scale around 1 day, but we cannot find an unambiguous interpretation for its light variations.

Key words. stars: oscillations – stars: variable: δ Scuti – stars: individual: AV Cet – stars: individual: HD 9139

1. Introduction

Among the most promising targets for successful application of asteroseismology are the δ Scuti stars. They have rich sets of oscillation modes which in many cases are readily observable. Unfortunately, each δ Scuti star is only found to oscillate in a seemingly random subset of possible modes, making it difficult to identify exactly which modes are observed. To further complicate matters, many of these stars are rapid rotators, which causes displacement of the frequencies. In fact, the proper treatment of rotation seems to be one of the major obstacles for real progress in our understanding of the δ Scuti stars.

In the last years, considerable effort has been expended to establish reliable mode identifications for a number of δ Scuti stars, but in most cases we are left with some ambiguity. Purely photometric techniques have the advantage of greater efficiency, and ultimately the ability to observe fainter stars than is possible with spectroscopy. A secure mode identification seems only possible if several techniques agree. Especially for rapidly rotating stars, there are too many free parameters and the understanding of rotation is too poor for one method alone to give a unique answer.

In this paper we present results on the fast rotating δ Scuti star AV Cet (HD 8511, F0V, $V = 6.21$, $v \sin i = 212$ km s^{-1}), discussing mode identification using both purely photometric techniques and a technique that combines simultaneous photometry and low dispersion spectroscopy.

The star AV Cet is a relatively poorly studied star, although it was recognised as a variable more than 30 years ago by Jørgensen et al. (1971). Gonzalez-Bedolla (1990) and Gonzalez-Bedolla et al. (1990) found one frequency interpreted as the fundamental mode, and also some evidence of another mode. From their short photoelectric light curves it is evident that the star is multiperiodic. The multiperiodicity was also evident from the line index variations of Hβ and Hγ, found by Dall & Frandsen (2002), from only four hours of spectroscopy. Despite the poor time coverage, the modes found by Gonzalez-Bedolla could be confirmed and moreover, evidence for more modes at higher frequencies was found. It was thus clear that the pulsational content of AV Cet was not secured and that more observations were needed.

In this paper we report a multi-observatory campaign conducted in October and November of 2001, aimed at establishing the main pulsational modes of AV Cet and, via spectroscopy and multicolour photometry, attempting a mode identification. This strategy is the same as was used by e.g. Viskum et al. (1998) and by Dall et al. (2002): by knowing the frequencies found from a photometric campaign, we can measure the amplitudes of the spectroscopic line indices of the Balmer lines Λ^{H}, without having to solve for the frequencies simultaneously. Moreover, we can compare the results from using different mode identification techniques.

Send offprint requests to: T. H. Dall, e-mail: tdall@eso.org
* Based partly on observations made with the Danish 1.5 m telescope at ESO, La Silla, Chile.

Table 1. Details on the telescopes and observations.

Observatory	Telescope diam. [cm]	Nights assigned/observed	Hours obtained	Remarks
ESO, La Silla	50	9/6	41.5	*uvby* photometry
SAAO, Sutherland	50	14/9	42.2	*vby* photometry
ESO, La Silla	154	9^a/6	35.4	spectroscopy

^{a} Granted 8 nights, but received half a non-photometric night from previous observer who needed photometric conditions.

2. Observations

In order to determine the frequency content of AV Cet and to be able to resolve modes with close frequencies, we needed long continuous photometric coverage. We observed in the Strömgren photometric filters in order to determine the pulsation periods, and the amplitudes in the *vby* bands, to be used for pulsation modelling and mode identification.

On the Danish 50 cm Strömgren Automatic Telescope (SAT) on La Silla we collected simultaneous *uvby* data with the four-channel photometer. On the 50 cm telescope at the South African Astronomical Observatory (SAAO), we acquired sequential *vby* data, excluding *u* because of its restricted use for mode identification of δ Scuti stars and to achieve denser data sampling.

With the Danish 1.54 m and DFOSC on La Silla, we had 8 nights of low resolution long slit spectroscopy. Resolution was around 6 Å with a 1.5″ slit, covering the Balmer lines from Hα to Hϵ. The CCD was windowed to improve the duty cycle, which with exposure times around 25–30 s was around 40%. These observations were carried out simultaneously with the photometric campaign.

Table 1 summarises the observations, which were all conducted between 24 Oct. and 4 Nov. 2001.

3. Data reduction

3.1. Strömgren photometry

The data from SAT and SAAO were reduced independently and later combined. For both data sets, we used HD 8070 (F2, $V = 6.6$) and HD 9139 (F5, $V = 6.7$) as comparison stars. It later turned out that HD 9139 is variable, and thus only HD 8070 was used as comparison. We will discuss the case of HD 9139 in Sect. 4.

The SAT data were reduced using the standard software developed at Copenhagen University Observatory. The reduction included airmass correction using standard extinction coefficients, and transformation to the standard photometric system.

The SAAO photometry was also reduced in a standard way. The correction for coincidence losses was followed by sky background subtraction. Nightly extinction coefficients were determined by means of the measurements of the constant comparison star HD 8070, and relative light curves of AV Cet and HD 9139 were computed with respect to HD 8070.

The timings were converted to Heliocentric Julian Date before combining the data sets from the two observatories.

3.2. Spectroscopy

The spectra were reduced using standard methods with IRAF[1].

After extraction of a spectrum, it was normalised to unity by dividing it by a fit to the sum of all the spectra. The spectra were neither wavelength calibrated nor flux calibrated, since the equivalent width (*EW*) and the line indices are relative quantities that are internally normalised by the continuum level. Consequently, they are not dependent on the precise intensity unit. Also, since we are looking for relative changes to this relative quantity, the amplitudes will be dimensionless, hence there is no need to convert pixel coordinates into true wavelength coordinates.

The line indices $\Lambda^{\rm H}$ were calculated for the Balmer lines Hα, Hβ, Hγ, and Hδ following the procedures described by Dall (2000) and applied by Dall et al. (2002) and Dall & Frandsen (2002). In short, a line index can be considered an analogue to a colour index, using software "filters" centered on the lines. The filters we have used are so-called super-Gaussians;

$$W = \exp\left(-\left(\frac{x - x_0}{b}\right)^8\right), \qquad (1)$$

where x_0 is the position of the line centre, and b is the HWHM. Note the exponent of 8.

4. HD 9139: An unclassified variable star

It was clear from the light curves that HD 9139 was not suited as a comparison star, and it is also clear that some seemingly periodic variations are the cause. A period analysis gives two dominant signals at 0.34 d^{-1} and 0.91 d^{-1}, but shows no signs of periods shorter than 1 day. However, there is a considerable amount of scatter at higher frequencies, which was why we were led to reject it as a comparison. We will discuss the cause of these variations in terms of damped pulsation, magnetic/rotational activity and nearby stellar companions.

The star is listed as F5 in SIMBAD with no indication of luminosity class. Also, no measurements of $v \sin i$ have been made so far.

HD 9139 was a target of the HIPPARCOS mission (ESA 1997), and Strömgren photometric indices are available from

[1] IRAF is distributed by the National Optical Astronomy Observatories, which are operated by the Association of Universities for Research in Astronomy, Inc., under cooperative agreement with the National Science Foundation.

the Lausanne-Geneva data base[2]. The calibrations of Crawford (1975) suggest the star is unreddened and has $M_v = 1.25 \pm 0.30$. It also seems metal-rich, as Nissen's (1988) calibration of the metallicity indicator δm_0 results in $[M/H] = 0.26$ for HD 9139. The HIPPARCOS parallax of the star implies $M_v = 1.68 \pm 0.23$, roughly in agreement with the absolute magnitude from the Strömgren colours. The model atmosphere calibrations of Kurucz (1991) then yield $T_{\rm eff} = 6850 \pm 100$ K and $\log g = 3.3 \pm 0.1$, which is near the red edge of the δ Scuti instability strip.

We have obtained high-resolution spectra of HD 9139 using the FEROS spectrograph on the ESO 1.52-m at La Silla Observatory. From the Fe I line at 4405 Å we estimate $v \sin i \sim 75$ km s^{-1}, hence a moderate rotation rate for a star at this position in the HR diagram. Comparison with spectra compiled by R. O. Gray[3] leads to a spectral type F5III-IV, based on the Ca II K line, the G-band, the strength of the Balmer lines, and the Ca I, Fe I and Mn I lines in the 4000–4400 Å range. The luminosity class was derived from the λ4077 Sr II and $\lambda\lambda$4172-8 Ti II, Fe II lines. This again places HD 9139 near the red edge of the instability strip, making it a δ Scuti or γ Doradus candidate. We plan to analyse the spectrum in detail and describe the characteristics in terms of basic parameters, abundances and $v \sin i$. With the knowledge of the abundance pattern we can try to sort out, whether the variability is due to a pulsational instability of some sort, due to magnetic effects (spots) coupled with rotation or due to some other phenomenon. This will be the subject of a later paper.

Using the abovementioned M_v and $T_{\rm eff}$ we can estimate a radius $R = 3.75\ R_\odot$ for HD 9139. The star then should have a fundamental radial mode period of ~1 day (corresponding to a pulsation constant $Q = 0.033$ d), which agrees with one of the two time scales found. This argues immediately against an interpretation of HD 9139 as a γ Doradus star, as those objects have high-order g-modes excited ($Q > 0.23$ d, Handler & Shobbrook 2002). We also note that, within the errors, the amplitudes of these two variations do not change significantly between the *vby* bands, which is inconsistent with pulsational variability.

Another possibility is magnetic activity on the star, implying an Ap (or Fp) spectral type, which would produce a rotationally modulated variation. We find from the derived value of $v \sin i$ an upper limit on the rotational period around 2.5 days, which within the errors agree with the 0.34 d^{-1} found. This would imply a near equator-on view of the star. However, we would still expect to see colour variation if the variation is due to surface abundance inhomogeneities. More importantly however, the spectrum of HD 9139 indicates that it is a normal F-star with no peculiar abundances.

The apparent variability might be explained by contamination from a nearby star, letting varying amounts of light into the diaphragm of the photometer, although this is expected to lead to shorter time scales. We do not find any likely contaminating source in the vicinity of HD 9139. The nature of HD 9139 and its variability thus is still not clear.

[2] http://obswww.unige.ch/gcpd/gcpd.html

[3] http://nedwww.ipac.caltech.edu/level5/Gray/frames.html

5. Time series analysis

As stated earlier, the spectroscopic analysis was never expected to deliver the mode frequencies, but only to provide amplitudes and phases in the line indices $\Lambda^{\rm H}$ to be used for mode identification.

The photometry on the other hand is crucial in establishing the frequency content of AV Cet, and also for providing amplitudes and phases for the mode identification. Below, we will describe first the analysis of the photometric data, and present the results. Next, with the resulting mode frequencies, we will derive amplitudes and phases for the line indices.

5.1. Strömgren photometry: Finding the mode frequencies

Before commencing the frequency analysis, both series were individually cleaned of deviant points, using a 4σ criterion, and then merged. Since there is no overlap between the two series, we avoid problems with distortion of the window function, caused by having higher weight in the overlap regions. The differences between the mean values of the two data sets in any filter are of the order of 0.3%. The correction of this offset was found to have no effect on the time series analysis.

The observing procedure at the SAT yielded one *uvby* data point every few minutes, largely oversampling the time series. Hence, we combined points in the SAT data, bringing the sampling of the two data sets closer, in order not to artificially weight one set more than the other. The combination was done using a weight based on the point to point scatter, multiplied by a time-difference sensitive Gaussian weight. Our optimisation lead to a re-sampling close to 11 min for the SAT data. This re-sampling was also found to be optimal with respect to S/N in the amplitude spectrum.

The weighting scheme applied here is the one recommended by Handler (2003), which is an improvement of a scheme used by e.g. Viskum et al. (1998) and Frandsen et al. (1995), using a weight proportional to σ^{-x}, where σ is an estimate of the internal scatter, and x in general is close to 1. The best value was in our case found to be $x = 0.9$, by optimising the final S/N in the amplitude spectrum. The internal scatter was calculated from a high-pass filtered series, and the weights were Fourier analysed to check for any periodicities; none were found.

The frequency analysis was done using Period98 (Sperl 1998) finding and prewhitening one frequency at a time, until no more peaks above 4σ were present in the amplitude spectrum. At each step care was taken to avoid errors due to aliasing, by checking also the ± 1 d^{-1} solutions. Finally, frequencies, amplitudes and phases were determined by a simultaneous fit around the final frequency table. The formal uncertainty on the frequencies is 0.05 d^{-1} from the total time span of the observations of 10.04 days. We estimated the additional errors introduced by underlying modes and aliases by applying several schemes of weighting and extraction of the frequencies

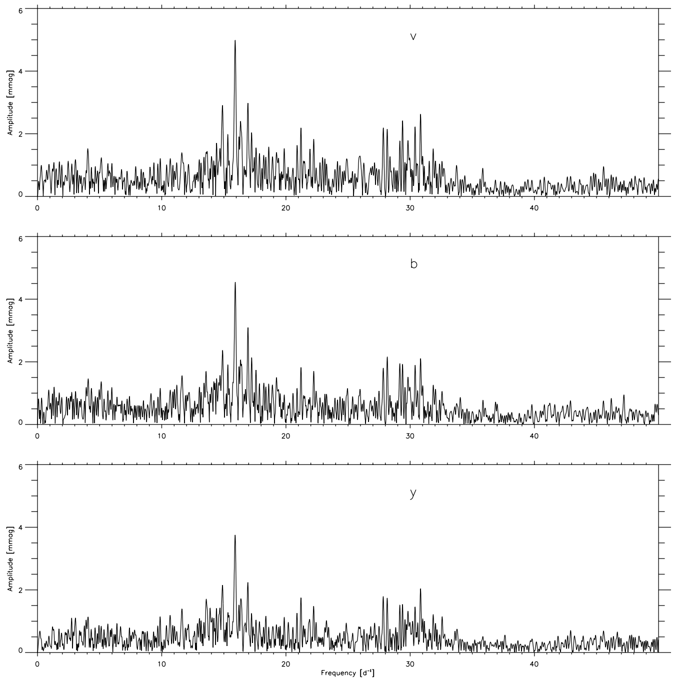

Fig. 1. The *vby* amplitude spectra of AV Cet.

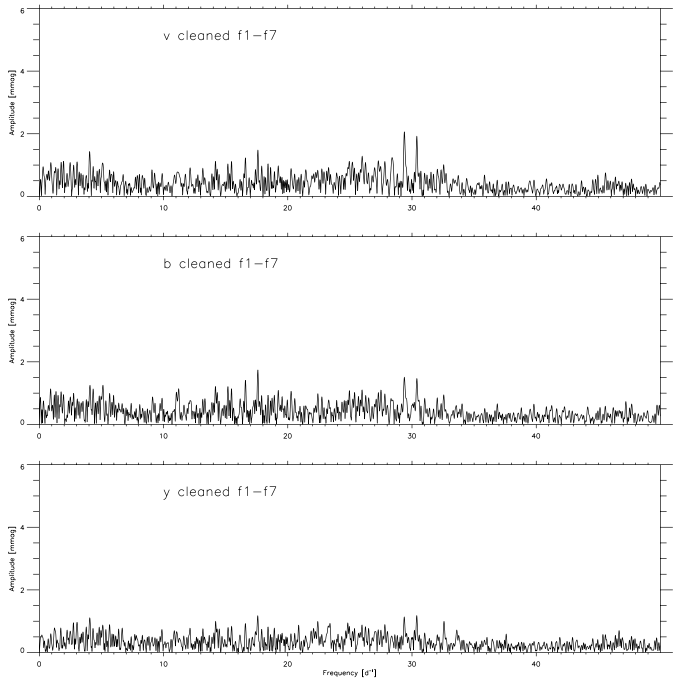

Fig. 2. The *vby* amplitude spectra of AV Cet after prewhitening with the frequencies f1–f7. There are quite evidently more modes present, most noticeable around 17 d^{-1} and 30 d^{-1} but these all have severe aliasing problems. See Table 2 and text for discussion.

Table 2. Modes detected in AV Cet. f1–f7 we regard as "safe", while the remaining modes all have some problems. See text for discussion.

ID	Frequency [d^{-1}]	Amplitude [mmag] v	b	y	S/N_v
f1	15.915	6.00 ± 0.44	5.46 ± 0.50	4.39 ± 0.36	13.6
f2	14.598	3.09 ± 0.43	2.96 ± 0.46	2.54 ± 0.34	7.2
f3	21.200	2.14 ± 0.48	1.76 ± 0.44	1.71 ± 0.40	4.5
f4	30.833	2.58 ± 0.54	2.01 ± 0.47	2.03 ± 0.37	4.8
f5	28.158	2.17 ± 0.64	2.12 ± 0.57	1.70 ± 0.46	3.4
f6	16.356	2.00 ± 0.47	1.69 ± 0.52	1.31 ± 0.37	4.3
f7	10.681	1.64 ± 0.39	1.38 ± 0.40	1.28 ± 0.33	4.2
The following modes are uncertain. See text for discussion.					
n8	17.59	1.49	1.75	1.19	
n9	14.19	1.03	1.14	1.00	
n10	30.38	1.91	1.39	1.17	

to the individual filters. The rms on the extracted frequencies was for all modes less than 0.01 d^{-1}, hence we adopt an error of 0.05 d^{-1} for the frequencies f1–f7 to be conservative. The results are summarised in Table 2. The amplitude spectra in the filters *vby* are shown in Fig. 1, while Fig. 2 show the corresponding spectra after removal of the frequencies f1–f7.

The errors on f1–f7 were calculated from the local residuals in the amplitude spectra after prewhitening with f1–f7. These errors do also include the contributions from n8–n10 and from any other undetected modes present. The noise level at frequencies above 40 d^{-1}, where the spectrum is essentially flat, was about a factor 2–2.5 better than the ones listed here, suggesting the presence of many unresolved low amplitude modes. Note that f5 is not detected above 4σ in any individual band ($S/N = 3.7$ in b and y). However, based on the collective evidence and on the fact that we find this mode above 4σ in all the line indices (Sect. 5.2), we have confidence in its reality.

The interpretation of the "modes" n8–n10 listed at the bottom of Table 2 is very problematic in such densely populated amplitude spectra. We do not feel confident about claiming accuracy or even reality for these modes, although they all stand out better than 4σ above the noise in at least one of the bands. Still, we find it worthwhile to list them for later reference. The inclusion of these modes in the solution for the amplitudes and phases, does not alter the solutions for f1–f7 noticeably.

For n8, we note that it is close to f2 + 3d^{-1}. On the other hand, it has significant amplitude, suggesting an independent mode interfering with the aliases of f2. The frequency of this mode however, must remain very uncertain given the large amount of unresolved modes evident in this region. The variations at frequency n9 may very well be an alias peak, and is merely included to show the level of unresolved power around this frequency. From Fig. 2 one may see two peaks around 30 d^{-1} separated by 1 d^{-1}. Whether this represents two modes interfering with each others aliases, or just a single mode (n10) is not clear.

5.2. Spectroscopic time series analysis

The calculation of the line indices involves choosing an integration filter for each line. This was done in the same way for all lines, finding the super-Gaussian filter that would optimise the S/N on the amplitude of f1.

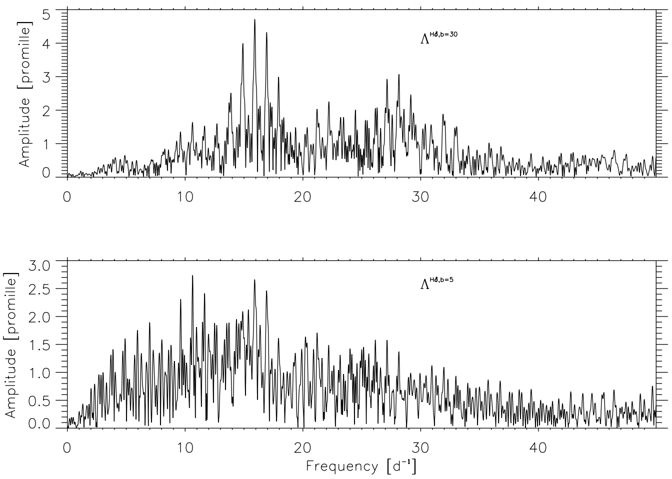

Fig. 3. Amplitude spectra of $\Lambda^{H\delta}$. The upper panel shows the amplitude spectrum for an integration filter including most of the line, while the lower one shows the result for a filter integrating only the core of the line.

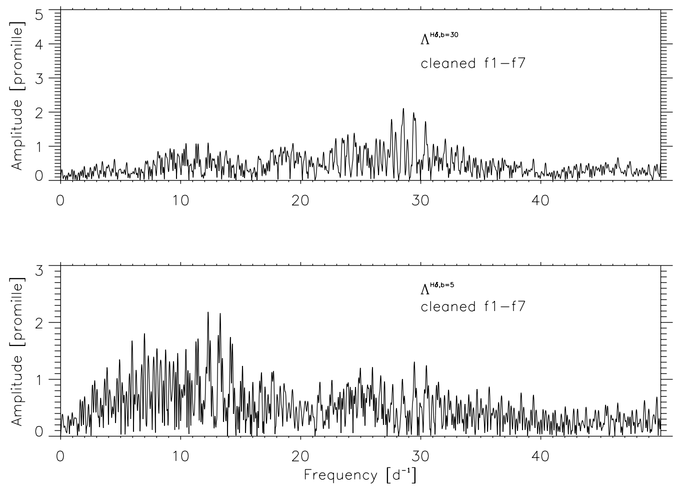

Fig. 4. Amplitude spectra of $\Lambda^{H\delta}$ after prewhitening with the frequencies f1–f7. The upper panel is for an integration filter including most of the line, while the lower panel shows the result for a filter integrating only the core of the line. As is evident, there are unresolved modes hidden in the noise.

Table 3. Results from prewhitening the line indices with f1–f7. All amplitudes are for the filter labelled b = 30 (Eq. (1)), except for $\Lambda^{H\delta,5}$ which lists the amplitudes in a filter that integrates only the core of the Hδ line. See text for discussion.

	Amplitude [promille][a]				
ID	$\Lambda^{H\beta}$	$\Lambda^{H\gamma}$	$\Lambda^{H\delta}$	$\Lambda^{H\delta,5}$	$S/N_{H\delta}$
f1	4.64 ± 0.50	5.27 ± 0.72	4.65 ± 0.40	3.09 ± 0.48	11.6
f2	1.78 ± 0.50	1.26 ± 0.72	1.78 ± 0.40	2.79 ± 0.42	3.0
f4	2.03 ± 0.73	2.14 ± 0.78	1.82 ± 0.75	1.11 ± 0.47	2.4
f5	3.08 ± 0.73	3.21 ± 0.79	3.13 ± 0.72	1.37 ± 0.49	4.1
f6	0.99 ± 0.50	2.00 ± 0.72	1.38 ± 0.40	1.71 ± 0.47	3.5
f7	0.99 ± 0.55	0.83 ± 0.71	0.99 ± 0.52	1.95 ± 0.66	1.9

[a] *Promille* is parts-per-thousand. One promille equals 1.086 mmag.

The line indices of the Balmer lines were analysed using the frequencies f1–f7 found in the Strömgren photometry as input. Before analysis the raw series was sigma-clipped to remove very deviant points. There were some obvious drifts in the series, which can often be removed by decorrelation with independent parameters that do not contain the pulsation signal. However, an investigation of external parameters like position of the spectrum on the CCD, seeing, continuum curvature etc. did not reveal any correlations or did not contain traces of the pulsational signal. Hence, we decided not to apply decorrelation to the series. Instead, the series was high-pass filtered to remove the drifts, while retaining the information in the (known) region of interest from ~8 d^{-1} and higher. Proper weights were constructed as outlined in the previous section.

The results from prewhitening with f1–f7 are summarised in Table 3. The amplitude spectrum, and the residuals after prewhitening are shown in Fig. 3.

As evident from Fig. 4 there are more modes excited in this star than the seven removed, which means that the accuracy of the amplitude determinations will suffer, as was the case for the photometry. The noise varies from ~0.6 promille around 10 d^{-1}, rising to ~0.8 promille at 30 d^{-1}, and levels out to around ~ 0.3 promille above 40 d^{-1}, which is the white noise level. Thus, the major contribution to the uncertainties comes from the unresolved modes, without which we would have gained up to a factor of 2.5 on the S/N.

Although the formal errors on the weaker modes are large, we can still have confidence in them since AV Cet is known to pulsate with these frequencies, found from the photometry.

In Table 3 we have listed the amplitudes of a Hδ line index $\Lambda^{H\delta,5}$ which is a very narrow integration filter that measures the amplitude in the core of the line. Note that f7 is significantly stronger here than in the line as a whole, meaning either that the variation is taking place only in the line core, or that the phase of the mode is changing between the core and the wings. Unfortunately, we do not have sufficient S/N to separate these two hypotheses, but an analysis of the line wings indicates that the mode is present but with a changing phase through the line. The other modes have a constant phase regardless of the position in the line.

We do not have a good model of the cause for this behaviour, but we might suggest that the nature of the mode is different from the other modes. The apparent presence of nodal lines in the phase suggests high m i.e. it could be a mode of $m \geq 2$. The low frequency of this signal lets us speculate that it could also be a g-mode or a mixed mode. Another explanation offered by Dall & Frandsen (2002) is that we see the effect of two very close unresolved modes, whose eigenfunctions are sampled differently at different depths of the atmosphere. As we have strong indications of many unresolved modes, this seems likely, although we do not have a precise model of such a scenario.

Table 4. Comparison between this work and earlier data. The formal errors on the GB amplitudes are 0.50 mmag.

ID	2001 y	1984 V
f1	4.39	2.61
f2	2.54	4.45
f3	1.71	2.41
f4	2.03	0.98
f5	1.70	1.21
f6	1.31	0.79
f7	1.28	0.78

5.3. Consistency with previous results?

The findings by Dall & Frandsen (2002) of three modes in AV Cet from four hours of line index measurements in Oct. 2000, can now be reassessed. Given the low frequency resolution many of the determinations are ambiguous, hence f1, f2 and f6 can not be disentangled. Fitting these three as a single mode, and keeping f3, f4, f5 and f7, we are able to fit the short data set very well. Notably, we find that the high frequency modes have amplitudes comparable to the main mode.

We have investigated the photoelectric data of Gonzalez-Bedolla (1990), to check if the modes we have found in our data from Oct. 2001 were also present in Sep. 1984. Gonzalez-Bedolla reported the dominant mode at 14.593 d^{-1} (our f2 mode) with another mode around 19.186 d^{-1} (likely to be our f3 mode). In Table 4 we present the results of a reanalysis of the data using our f1–f7. As Gonzalez-Bedolla, we find f2 to be dominant with f1 and f3 also present. The modes f4–f7 are not present above the 4σ level. Hence, no measurable high frequency modes were present in 1984, and thus there was significant redistribution of the pulsational energy in the course of 16 years, possibly including amplitude variations and excitation of new modes.

6. Discussion

6.1. Temperature and luminosity of AV Cet

The discussion of the pulsational behaviour of AV Cet requires some knowledge of the star's position in the HR diagram. As AV Cet was both a target of the HIPPARCOS mission (ESA 1997) and as standard photometric colours in both the Strömgren and Geneva systems are also available[4], its effective temperature and luminosity can be determined.

The calibrations of the Strömgren system by Crawford (1979) applied to AV Cet suggest that the star is unreddened, slightly metal deficient ($\delta m_0 = 0.016$) and that it has an absolute magnitude $M_v = 2.1 \pm 0.3$. This is in excellent agreement with the HIPPARCOS result: $\pi = 14.83 \pm 0.77$ mas combined with $V = 6.21$ gives $M_v = 2.07 \pm 0.12$. Smalley's (1993) calibration in terms of metallicity suggests $[M/H] = -0.09$ for AV Cet and the model atmosphere grids by Kurucz (1991) imply $T_{\rm eff} = 7820$ K as well as $\log g = 4.1$.

[4] http://obswww.unige.ch/gcpd/gcpd.html

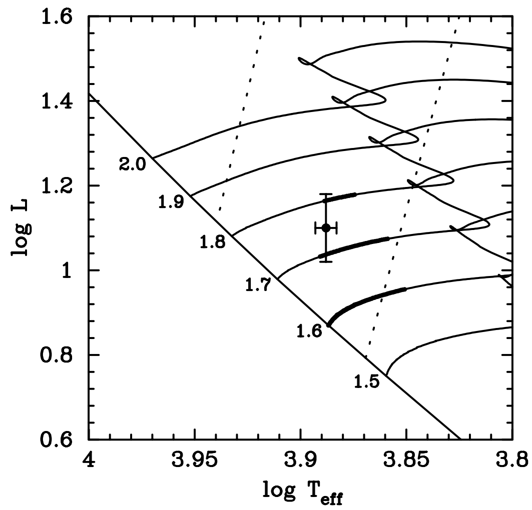

Fig. 5. AV Cet in the theoretical HR diagram. The filled circle shows the temperature and luminosity constraints we derived; error bars on these determinations are indicated. Stellar evolutionary tracks for models with $[Z] = 0.015$ and $v_{\rm rot,ZAMS} = 250$ km s^{-1} are indicated and labelled with their masses. The slanted solid line depicts the ZAMS for these models, and the slanted dotted lines are the edges of the δ Scuti instability strip. The thick sections of the evolutionary tracks correspond to models whose range of unstable pulsational frequencies matches that of AV Cet.

Applying the calibration of Geneva photometry by Künzli et al. (1997) to AV Cet, we find $T_{\rm eff} = 7650$ K, $\log g = 4.0$ as well as $[M/H] = -0.2$, which is in good agreement with the outcome from the application of the Strömgren colour calibrations. Consequently, we adopt $T_{\rm eff} = 7730 \pm 90$ K as our temperature estimate, and with the bolometric corrections by Flower (1996) and Drilling & Landolt (2000) we find $M_{\rm bol} = 2.0 \pm 0.2$.

To place AV Cet in a theoretical HR diagram, its projected rotational velocity is also required. Two determinations are available from the literature: Abt & Morrell (1995) determined $v \sin i = 195$ km s^{-1}, and Royer et al. (2002) measured $v \sin i = 212$ km s^{-1}. As this is close to the break-up rotational velocity of a main-sequence A star, we must see AV Cet close to equator-on.

We computed evolutionary sequences of stellar models with the Warsaw-New Jersey code (see e.g. Pamyatnykh et al. 1998 for a description). Owing to the observational constraints determined above, we chose models with a heavy-element abundance $[Z] = 0.015$ and a rotational velocity of $v_{\rm rot} = 250$ km s^{-1} on the ZAMS. No convective core overshooting was used. We compare these tracks with the temperature and luminosity of AV Cet in Fig. 5.

It is suggested that AV Cet is a star of $1.75 \pm 0.06\, M_\odot$ about halfway in its main sequence evolutionary phase. We can check this finding with the application of a pulsational stability analysis (as explained by Pamyatnykh 2003). In brief, the range of unstable pulsation frequencies of a given pulsational model changes as it evolves. This frequency range can be matched with the one actually observed in the star. We have applied this method to AV Cet (taking into account rotational splitting due to fast rotation as well) along the evolutionary tracks plotted in Fig. 5, where models that reproduce the observed frequency range with their $\ell = 0-2$ modes are located along the thick parts of the tracks. We find very good agreement between the parameter space occupied by those models and the observationally determined position of AV Cet in the HR diagram. The modes excited in the models that match our constraint on the temperature from the colour photometry range from (almost) pure g modes that start as g_3 on the ZAMS through mixed modes up to pure p modes of radial order 5.

However, since such a fast rotating star will be highly flattened with many complicated phenomena going on like mixing, meridional circulations etc., we do not expect any current state-of-the-art models to fully describe AV Cet.

6.2. On mode identifications

As is evident from Figs. 2 and 4, we have not succeeded to extract all the pulsation modes that our formal accuracy would have allowed us to, mostly because of severe aliasing problems in regions very densely populated with unresolved modes. This is true both for the Strömgren photometry and for the line index spectroscopy, and it may even be different modes that dominate the residuals. As there is still substantial power left we can not expect to be able to make very accurate mode identifications based on amplitude ratios and phase differences.

Nevertheless, we present in Fig. 6 some mode identification plots suggested in the literature. Without attempting any definite mode identification, we will in the following compare the methods and discuss whether they collectively can point to any conclusions.

In the Viskum-diagram (e.g. Viskum et al. 1998, upper left-hand side panel of Fig. 6) the modes are grouped according to their spatial structure, i.e. to their ℓ or m values, with low-ℓ, m in the lower left and high-ℓ, m towards the upper right. This plot does indeed seem to indicate groupings, leading to f2 and f7 being radial modes. Alternatively, given the large errors on f7, its special phase values in Fig. 6 and its low frequency, a better interpretation is that f7 is a low degree ($\ell = 1$) g-mode. As discussed by Dall & Frandsen (2002), radial modes in δ Scuti stars seem to fall near amplitude ratios of 0.5, in support of the interpretation of f2 being radial. However, error bars are large. Certainly, the Viskum diagram has been used with success for a number of pulsating stars of various classes in recent years; (apart from FG Vir, the most notable are the roAp star α Cir, Baldry et al. 1998, 1999 and the EC 14026 star PG 1605+072, O'Toole et al. 2003). However, it is very likely that in the regime of very fast rotation, the geometrical properties on which the method relies are so heavily distorted that the interpretation is no longer correct. For the moderately fast rotator BN Cnc, Dall et al. (2002) discussed the interpretation of the amplitude ratios, noting that for such fast rotation the ratios would depend largely on m in combination with the inclination angle because of the large amount of gravity darkening in addition to the limb darkening. Thus, we would need to know the rotation period and $v \sin i$ independently. The modes with low amplitude ratios would nevertheless still have the smallest amount of spatial structure, so if we were to look for any radial modes, we would have to look among these modes. In the case of AV Cet, this means that if the star has radial modes, they would likely be found among the modes f2 and f7.

The multi-colour photometric method has been very successful in the past, using the Garrido-diagram (Garrido et al. 1990). One of the most serious shortcomings in this case is the lack of understanding of the effects of fast rotation, and of models able to take those into account. Such models would be necessary to assign "regions of interest" for specific values of ℓ within the diagram. But even if such models were at hand, the effort would be unfruitful because of the high rotation rate of AV Cet, which would cause the "regions of interest" to be not only inaccurate, but also to a great extent overlapping, hence making any identifications ambiguous. It is worth noting the large range in phase difference for AV Cet: for most other stars $\phi_{b-y} - \phi_y$ spans no more than 50°, while here we have a range of at least 200°, and even if we disregard the most uncertain point (f7), the range is more than 100°.

In the case of FG Vir, Breger et al. (1999) pointed out the very good agreement between the Garrido-diagram and the Viskum diagram in determining the ℓ values for the strongest modes of FG Vir. In the diagram presented by Breger et al., the modes are clearly grouped along a line of negative slope. One grouping corresponding to the radial modes was located at low $A(\mathrm{H})/A(v)$ and $\phi_v - \phi_y \sim 2°$, while high-ℓ modes were grouped at high $A(\mathrm{H})/A(v)$ and $\phi_v - \phi_y \sim -7°$. Only if we take the errors into consideration in the Breger-diagram of AV Cet do we find some resemblance, which would then indicate high spherical degree for the f3 mode, while the rest would have considerable ambiguity.

Without making any physical assumptions, Paparo & Sterken (2000) tested all possible combinations of photometric amplitude ratios and phase differences for the groupings of modes, that might be useful for mode identification in the star θ Tuc. They found that the combination $A(b)/A(y)$ versus $\phi_{b-y} - \phi_b$ was particularly useful for separating modes of different degree and radial order without giving any exact assignments to particular groups. The corresponding Paparo/Sterken-diagram for AV Cet may indeed show some separations. Following the interpretation of the phase difference reflecting the degree, we may here see at least three different groupings, with f7 belonging to the lowest one. If we exclude f7, the mode with the highest positive phase difference is f2, which we already suspected as the radial mode. The errors on the amplitude ratios are quite high, and do not allow us to suggest any groupings. As with the Garrido-diagram the phase differences span a large range: here the modes cover at least 100°, while for θ Tuc the range was ~35°.

7. Conclusions

We have found a previously unknown variable star, HD 9139, the nature of which is still unclear. Under a pulsational hypothesis, the Q-value disagrees with an interpretation of HD 9139

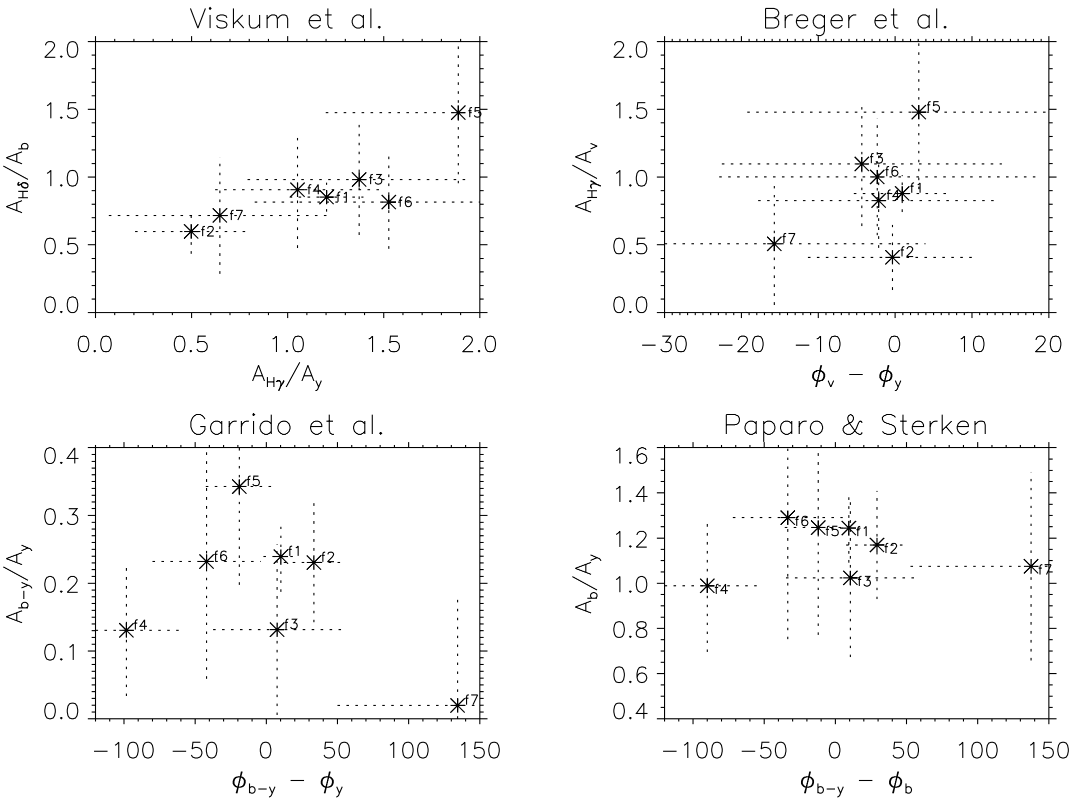

Fig. 6. The different mode identification plots suggested in the literature. The top left plot is the one used by Viskum et al. (1998) and Dall et al. (2002), while the top right one is the plot used by Breger et al. (1999) to demonstrate the good agreement in the case of FG Vir between the method of Viskum et al. and the photometric method – which is the plot on the lower left (Garrido et al. 1990). The lower right plot is similar to that empirically suggested by Paparo & Sterken (2000) for θ Tuc.

as a star of the γ Doradus type, but the star could be a δ Scuti star just leaving the instability strip.

Another explanation may be abundance inhomogeneities, possibly induced by magnetic activity, which coupled with rotation produces the variation. The spectrum seems however to indicate a normal F star. Both scenarios are somewhat limited by the absence of amplitude variations with colour.

The rapidly rotating δ Scuti star AV Cet has turned out to be an extremely interesting object. From this observing campaign we find seven individual pulsation modes with good evidence for more, and from comparison with old data, we see significant redistribution of pulsational energy, suggesting that the star has undergone amplitude variations and excitation of new modes during the course of 16 years.

The fast rotation is the main cause of the difficulties involved in establishing secure mode identifications for this star. We have compared several methods previously used for other δ Scuti stars, but find that none of them provides any clear interpretation of the mode nature. Based on the collective evidence, we do however propose the mode f2 = $14.598\,\mathrm{d}^{-1}$ as our best candidate to be radial based on the tendency for low degree modes to give small amplitude ratios in the Viskum diagram. This is supported by the positive phase difference $\phi_{b-y} - \phi_y$. Likewise, we suggest that f5 = $28.158\,\mathrm{d}^{-1}$ may be a high-degree ($\ell = 2$–3) mode, based on the high amplitude ratios demonstrated by the Viskum-, Breger-, and Garrido-diagrams. We also suggest that the mode f7 = $10.68\,\mathrm{d}^{-1}$ may be a mode of $m \geq 2$ and/or a low order g-mode, based on the peculiar behaviour in the line profile of the Balmer lines, and on its very large phase differences, which point to a different mode nature.

We have shown that the various diagrams used for mode identification show significant differences between the seven detected modes. The interpretation is difficult due to the fast rotation of AV Cet, although one gets an idea about the division of the modes in low and high spatial structure modes. A better theoretical understanding of the effects of rotation on observable parameters is needed. AV Cet is a highly interesting target for further studies in this direction because of its unevolved nature and its large number of observable pulsation modes.

Acknowledgements. We wish to thank L. F. Olesen for giving us half a night of her assigned observing time at the Danish 1.54 m. This research was supported by the Danish Natural Science Research Council through its centre for Ground-Based Observational Astronomy, IJAF. This research has made use of the SIMBAD database, operated at CDS, Strasbourg, France.

References

Abt, H., & Morrell, N. I. 1995, ApJS, 99, 135

Baldry, I. K., Bedding, T. R., Viskum, M., et al. 1998, MNRAS, 295, 33

Baldry, I. K., Viskum, M., Bedding, T. R., et al. 1999, MNRAS, 302, 381

Breger, M., Pamyatnykh, A. A., Pikall, H., & Garrido, R. 1999, A&A, 341, 151
Crawford, D. L. 1975, AJ, 80, 955
Crawford, D. L. 1979, AJ, 84, 1858
Drilling, J. S., & Landolt, A. U. 2000, in Allen's Astrophysical Quantities, 4th ed., ed. A. N. Cox (Springer Verlag), 392
Dall, T. H. 2000, in NOT in the 2000's, ed. N. Bergvall, L. O. Takalo, & V. Piirola (Univ. of Turku), 54
Dall, T. H., & Frandsen, S. 2002, A&A, 386, 964
Dall, T. H., Frandsen, S., Lehmann, H., et al. 2002, A&A, 385, 921
ESA 1997, The Hipparcos and Tycho catalogues, ESA SP-1200
Flower, P. J. 1996, ApJ, 469, 355
Frandsen, S., Jones, A., Kjeldsen, H., et al. 1995, A&A, 301, 123
Garrido, R., Garcia-Lobo, E., & Rodriguez, E. 1990, A&A, 234, 262
Gonzalez-Bedolla, S. 1990, Rev. Mex. A&A, 21, 401
Gonzalez-Bedolla, S., Rolland, A., Rodríguez, E., & Lopez de Coca, P. 1990, IBVS, 3533
Handler, G., & Shobbrook, R. R. 2002, MNRAS, 333, 251
Handler, G. 2003, Balt. Astron., 12, 253
Jørgensen, H. E., Johansen, K. T., & Olsen, E. H. 1971, A&A, 12, 223
Künzli, M., North, P., Kurucz, R. L., & Nicolet, B. 1997, A&AS, 122, 51
Kurucz, R. L. 1991, Van Vleck Obs. Contr., 11, 27
Nissen, P. E. 1988, A&A, 199, 146
O'Toole, S. J., Jørgensen, M. S., Kjeldsen, H., et al. 2003, MNRAS, 340, 856
Pamyatnykh, A. A. 2003, in Asteroseismology Across the HR Diagram, ed. M. J. Thompson, M. S. Cunha, & M. J. P. F. G. Monteiro (Kluwer), in press
Pamyatnykh, A. A., Dziembowski, W. A., Handler, G., & Pikall, H. 1998, A&A, 333, 141
Paparó, M., & Sterken, C. 2000, A&A, 362, 245
Royer, F., Grenier, S., Baylac, M.-O., Gomez, A. E., & Zorec, J. 2002, A&A, 393, 897
Smalley, B. 1993, A&A, 274, 391
Sperl, M. 1998, Comm. Asteroseismol., 111, 1
Viskum, M., Kjeldsen, H., Bedding, T. R., et al. 1998, A&A, 335, 549